bioRxiv preprint doi: https://doi.org/10.1101/343640; this version posted June 11, 2018. The copyright holder for this preprint (which was not certified by peer review) is the author/funder, who has granted bioRxiv a license to display the preprint in perpetuity. It is made available under aCC-BY-NC 4.0 International license.

Culturing the ubiquitous freshwater actinobacterial acI lineage by supplying a biochemical 'helper' catalase

Suhyun Kim†, Ilnam Kang†, Ji-Hui Seo, and Jang-Cheon Cho*

Department of Biological Sciences, Inha University, Incheon 22212, Republic of Korea

† These authors contributed equally to this work.

*E-mail: chojc@inha.ac.kr

Corresponding author information:

Address: Department of Biological Sciences, Inha University, Inharo 100, Namgu, Incheon 22212, Republic of Korea

Tel: +82-32-860-7711

bioRxiv preprint doi: https://doi.org/10.1101/343640; this version posted June 11, 2018. The copyright holder for this preprint (which was not certified by peer review) is the author/funder, who has granted bioRxiv a license to display the preprint in perpetuity. It is made available under aCC-BY-NC 4.0 International license.

Unlike the ocean from which abundant microorganisms with streamlined genomes such as *Prochlorococcus*[1], *Pelagibacter*[2], and *Nitrosopumilus*[3] have been isolated, no stable bacterial cultures are available for the ubiquitous freshwater actinobacterial acI lineage[4]. The acI lineage is among the most successful limnic bacterioplankton found on all continents[5], often representing more than half of all microbial cells in the lacustrine environment[6,7] and constituting multiple ecotypes[5,8]. Dilution-to-extinction culturing followed by whole-genome amplification recently yielded 20 complete acI genomes from lakes in Asia[9] and Europe[10]. However, the establishment of stably growing cultures has failed despite various cultivation efforts[9-13] using growth factors predicted from genome information[14]. Here, we report two pure cultures of the acI lineage successfully maintained by supplementing catalase into the growth media. Catalase was critical for stabilizing growth by degrading hydrogen peroxide irrespective of the genomic presence of the catalase-peroxidase (*katG*) gene, making the acI strains the first example of Black Queen Hypothesis[14] reported for freshwater bacteria. The two strains, representing two novel species, displayed differential phenotypes and distinct preferences for reduced sulfurs and carbohydrates, some of which were difficult to predict based on genomic information. Our results suggest that culturing the hitherto-uncultured freshwater bacteria can be facilitated by the simple catalase-supplement method and indicate that genome-based metabolic prediction can be complemented by physiological analyses.

In contrast to the typical terrestrial *Actinobacteria* found in soil and sediments, planktonic acI *Actinobacteria* have streamlined genomes[15] with 1.2–1.6 Mb genome sizes and are predicted to show auxotrophy for vitamin B compounds, some amino acids, and reduced sulfurs[8-10,16]. Despite the rich genomic data obtained from putatively axenic cultures and various cultivation efforts driven by genomic information, all initial cultures have been lost and no growing cultures are currently available[9,10], preventing further ecological studies on the ubiquitous acI lineage. In the present study, we successfully cultivated the acI lineage by catalase supplementation to remove hydrogen peroxide.

Strain IMCC25003 of the acI-A1 tribe and strain IMCC26103 of the acI-A4 tribe[4,5] were isolated from Lake Soyang in Korea by dilution-to-extinction culturing[9]. Strains IMCC25003 and IMCC26103 were most closely related to the recently proposed Candidatus species '*Ca*. Planktophila sulfonica' MMS-IA-56 (100%) and '*Ca*. Planktophila lacus' MMS-21-148 (99.9%)[10], respectively, based on their 16S rRNA gene phylogenetic

bioRxiv preprint doi: https://doi.org/10.1101/343640; this version posted June 11, 2018. The copyright holder for this preprint (which was not certified by peer review) is the author/funder, who has granted bioRxiv a license to display the preprint in perpetuity. It is made available under aCC-BY-NC 4.0 International license.

analyses (Supplementary Fig. 1). According to the average nucleotide identity (ANI)[17] with their closest relatives (74–86%)[10], the two strains each represent novel species of the genus '*Ca*. Planktophila'.

Because the two strains were among the few acI isolates and the ability to maintain stably-growing acI strains is prerequisite to studying the phenotypic characteristics of the acI lineage, we first attempted to resuscitate both strains from glycerol stocks. IMCC26103 did not grow for 21 days after reviving from the original frozen glycerol stocks but showed an abrupt increase in cell density (Supplementary Fig. 2a), which was found to be due to the growth of contaminating strains (Supplementary Fig. 2b). IMCC25003 began growing without a lag from the original frozen stocks and reached a cell density of 7.6×10^5 cells ml^{-1} in 5 days (Supplementary Fig. 2c; upper panel), but showed an atypical growth curve when the revived culture was transferred into the same medium on day 12 (Supplementary Fig. 2c; middle panel). When the first-transferred culture was inoculated again on day 15, no growth was detected until ~70 days (Supplementary Fig. 2c; lower panel). Because maintenance of the growing cultures of the acI strains was not successful in the media used for their original isolation, further attempts to obtain stable cultures were made by introducing various modifications to the media composition. These attempts were possible only for IMCC25003, as many glycerol stocks could be stored using the firstly revived cultures of IMCC25003. Modification of media composition was based on the putative metabolic features and growth requirements of the acI lineage predicted by approaches such as microautoradiography combined with fluorescence *in situ* hybridization (FISH) and single-cell genomics[8,18]. Culture media contained various supplements of FAMV medium (*see* Supplementary Table 1 for media composition) such as carbon substrates, proteinogenic amino acids, peptone, and yeast extract and different basal media including artificial freshwater medium (AFM)[19] and spent medium of *Limnohabitans* sp. IMCC26003 (Supplementary Table 2). However, growth of IMCC25003 was not detected under any culture conditions tested.

Failure in establishing stable acI bacterial cultures by supplementation with defined or undefined nutrients led us to hypothesize that controlling the putative growth inhibitors may be more crucial than supplying growth promoters. Because the growth of *Prochlorococcus* and ammonia-oxidizing archaea (AOA) was previously found to be promoted by removing hydrogen peroxide (H_2O_2)[20-22], we examined whether catalase, an enzyme that degrades H_2O_2, could facilitate the cellular growth of IMCC25003, although the IMCC25003 genome contains *katG*, which codes for a bifunctional catalase-peroxidase. IMCC25003 showed good growth and reached a maximum cell density of 2.7×10^7 cells ml^{-1} in catalase (10 U ml^{-1})-amended medium

bioRxiv preprint doi: https://doi.org/10.1101/343640; this version posted June 11, 2018. The copyright holder for this preprint (which was not certified by peer review) is the author/funder, who has granted bioRxiv a license to display the preprint in perpetuity. It is made available under aCC-BY-NC 4.0 International license.

(FAMV+CM+AA, *see* Methods for media composition), while no growth was detected in the medium devoid of catalase (Supplementary Fig. 3a). IMCC26103, which does not contain *katG*, was also successfully revived from the last-remained glycerol stocks in the catalase-amended medium, attaining a maximum cell density of 5.2×10^7 cells ml^{-1} (Supplementary Fig. 3b). Because both strains exhibited robust and reproducible growth upon repeated transfers in the media supplemented with catalase, catalase was considered a critical supplement in acI strain cultivation.

Before further experiments, dilution-to-extinction culturing of the successfully revived strains was performed twice to ensure the purity of the cultures, resulting in the establishment of stably growing pure cultures. The purity of the established cultures was verified by FISH (Fig. 1a), transmission electron microscopy (Fig. 1b), and whole genome sequencing followed by read mapping. Both strains produced reddish cell pellets colored by carotenoids and actinorhodopsin in 4 L cultures (Supplementary Fig. 4a), which were subsequently used for genome sequencing. The genome sequences were identical (1 base pair difference) to those obtained by multiple displacement amplification (MDA) in our previous study[9], with more even sequencing coverages (Supplementary Fig. 4b). For both strains, more than 99.9% of sequencing reads were mapped to the complete genomes, demonstrating the purity of the cultures.

To reconfirm the catalase-dependent growth, the two acI strains were cultivated with various concentrations of catalase (0–20 U ml^{-1}). Growth of the strains was dependent on the presence of catalase, as no growth was detected in the absence of catalase, while 0.5 U ml^{-1} catalase increased the cell density to ~10^7 cells ml^{-1} (Fig. 2a, b). Cell densities and H_2O_2 concentrations were simultaneously monitored in a catalase-spiked growth experiment to determine whether the pivotal role of catalase in promoting growth is mediated by degradation of H_2O_2. Without catalase, no cellular growth was detected (Fig. 2c, d) and the H_2O_2 concentration was maintained at the initial level of ~60 nM (Fig. 2e, f). In contrast, when 10 U ml^{-1} catalase was added at the time of inoculation, the H_2O_2 concentration decreased promptly to less than 10 nM and the acI strains began growing, reaching maximum cell densities in 6–9 days. When catalase was spiked at 7 or 13 days for IMCC25003 and 5 or 12 days for IMCC26103, the H_2O_2 concentration rapidly decreased from ~60 nM to ~10 nM (Fig. 2e, f). The acI strains, which showed no growth before catalase addition, began growing following the decrease in H_2O_2 concentration immediately after catalase addition, indicating that H_2O_2 removal by catalase was critical for maintaining the growth of the acI strains.

bioRxiv preprint doi: https://doi.org/10.1101/343640; this version posted June 11, 2018. The copyright holder for this preprint (which was not certified by peer review) is the author/funder, who has granted bioRxiv a license to display the preprint in perpetuity. It is made available under aCC-BY-NC 4.0 International license.

Among the several traits explained by the Black Queen Hypothesis (BQH)[14] such as auxotrophy for vitamins or amino acids[15,23], the dependency on external H_2O_2 scavengers is the first-reported and among the most representative cases of the BQH, discovered in two abundant marine autotrophic prokaryotic groups, *Prochlorococcus* and AOA[20-22]. The dependency of cellular growth on the external H_2O_2 scavenger found in this study makes the acI lineage the first freshwater bacterial example supporting the BQH, which explains the evolution of metabolic dependency of genome-streamlined oligotrophic bacteria on external 'helpers' in nutrient-depleted environments[15,24]. This crucial role of catalase in cultivating the acI strains was rather unexpected because all culture media used in cultivation trials contained pyruvate, a well-known chemical scavenger of H_2O_2[25,26] and because acI bacteria failed to resuscitate from the original dilution cultures regardless of the presence of *katG*[9,10]. In this context, we first assumed that some unknown growth factors would be required for laboratory cultivation rather than H_2O_2 scavengers and tested various nutrients and growth factors to revive the acI strains. However, only catalase treatment resulted in successful cultivation of the acI strains, while all other attempts failed. Our cultivation results suggest that acI bacteria grow only at very low concentrations of H_2O_2 attainable by catalase addition under laboratory conditions, regardless of the presence of *katG*, suggesting that the metabolic dependency of bacterial groups cannot be predicted based solely on genome information.

Although *katG* was found only in IMCC25003, the two acI strains showed similar growth responses to H_2O_2: no growth at a high concentration of H_2O_2 but good growth at minute concentration of H_2O_2 lowered by catalase. This result indicated that the *katG* gene of IMCC25003 or its gene product, bifunctional catalase-peroxidase (KatG), did not function properly in defense against H_2O_2 in the culture expriments. Therefore, we first examined expression of *katG* in IMCC25003 by qPCR. The qPCR results showed that *katG* was expressed and the relative expression level increased slightly with increasing H_2O_2 concentrations (Supplementary Fig. 5). Next, *katG* of IMCC25003 was cloned and expressed in *E. coli* and the gene product was purified by affinity chromatography (Supplementary Fig. 6). The native molecular weight of IMCC25003 KatG was ~165 kDa (Supplementary Fig. 6d) and the molecular weight of the subunit analyzed by SDS-PAGE was ~83 kDa (Supplementary Fig. 6a), indicating that IMCC25003 KatG formed a homodimer composed of two subunits. In an in-gel enzyme activity assay, IMCC25003 KatG showed both catalase and peroxidase activities but its catalase activity was much lower than that of bovine catalase (KatE), belonging to the monofunctional catalase group, which was supplemented into the culture media in this study (Supplementary Fig. 7). To more accurately

bioRxiv preprint doi: https://doi.org/10.1101/343640; this version posted June 11, 2018. The copyright holder for this preprint (which was not certified by peer review) is the author/funder, who has granted bioRxiv a license to display the preprint in perpetuity. It is made available under aCC-BY-NC 4.0 International license.

assay catalase activity of IMCC25003 KatG, decomposition of H_2O_2 was plotted using varying amounts of enzymes (Supplementary Fig. 8). All enzymatic parameters including specific activity (U mg^{-1}) and catalytic efficiency (k_{cat}/K_m) showed that IMCC25003 KatG displayed lower catalase activities than those of other microbial KatGs reported previously as well as bovine catalase (KatE) assayed in this study (Supplementary Table 3), suggesting that IMCC25003 KatG does not have an activity sufficient to overcome the growth inhibition by H_2O_2 present in the culture media.

We investigated the distribution of *katG* among the acI genomes available, as only one (IMCC25003) of four acI strains isolated from Lake Soyang contains *katG*[9]. *katG* was found in 14 of 20 complete acI genomes (Supplementary Table 4). When single amplified genomes were included, 20 of 35 genomes carried *katG*. The distribution of *katG* in the acI lineage was biased toward acI-A compared to acI-B. Of the 25 acI-A genomes 19 carried *katGs*, while only one of 10 acI-B genomes contained *katG* (Supplementary Table 4), which prompted us to analyze phylogenetic features of acI KatG proteins. Unexpectedly, phylogenetic analyses including diverse bacterial KatG proteins[27] indicated that KatGs of the acI lineage belonged to two distinct groups that are separated widely in the entire KatG tree (Fig. 3a). Further, this KatG phylogeny of the acI lineage was not consistent with a phylogenomic tree of the lineage based on conserved proteins (Fig. 3b). KatGs of the acI-A sublineage were divided into two different KatG groups depending on the tribes. acI-A1 and A2 KatGs formed group A, while acI-A4, A5, A6, and A7 KatGs formed group B together with KatG of acI-B4 (Fig. 3). These results indicate that complicated evolutionary processes occurred for KatG in the acI lineage. Because KatG of IMCC25003 belonging to the group A showed a low activity, it would be interesting to see determine KatGs belonging to group B also exhibit low catalase activity, as isolates possessing group B KatG were also reported not to grow in lake water-based medium[10].

Establishment of stable pure cultures by catalase addition enabled the first phenotypic characterization of the acI lineage which may have been impossible without cultures, including detailed morphology (Fig. 1b), temperature preference (Supplementary Fig. 9), fatty acid profile (Supplementary Table 5), growth requirement, and substrate utilization (Fig. 4), leading to the proposal of two novel species named as '*Ca*. Planktophila rubra' for IMCC25003 and '*Ca*. Planktophila aquatilis' for IMCC26103 (*see* Supplementary Text). Actively growing cells of the two strains were curved rods of very small sizes and biovolumes of 0.041 (for IMCC25003) and 0.061 μm^3 (for IMCC26103), representing one of the smallest ultramicrobial (<0.1 μm^3) cells among known

bioRxiv preprint doi: https://doi.org/10.1101/343640; this version posted June 11, 2018. The copyright holder for this preprint (which was not certified by peer review) is the author/funder, who has granted bioRxiv a license to display the preprint in perpetuity. It is made available under aCC-BY-NC 4.0 International license.

cultivated freshwater bacteria, but 1.6–2.4-fold larger cell volumes than those of other acI bacteria estimated by epifluorescence microscopy[10] (Supplementary Table 6).

The cell densities of IMCC25003 were increased by amino acids but not by carbon mixtures (Fig. 4a). Growth of IMCC26103 was enhanced by both amino acids and carbon mixtures, but the enhancement by carbon mixtures was observed only in the presence of amino acids (Fig. 4b). These results indicated that the growth of both strains was mainly limited by at least one of 20 amino acids and that IMCC26103 (but not IMCC25003) utilized at least one of the carbon sources added. In each carbon compound-amended experiment, no single carbon compound affected the growth of IMCC25003 (Fig. 4c), but ribose and glucose enhanced the growth of IMCC26103 (Fig. 4d). These results were supported by genomic information showing that the IMCC26103 genome contained genes for D-ribose pyranase, ribokinase, and glucose ABC transporter, while none of these genes were found in the IMCC25003 genome. In each amino acid-amended test, methionine and cysteine increased the growth of both strains (Fig. 4e, f), supporting the genome-based metabolic prediction that acI strains lacked the assimilatory sulfate reduction pathway and thus require reduced sulfur compounds for growth[9]. Interestingly, the two strains showed different preferences for reduced sulfur compounds. IMCC25003 preferred methionine (optimum at 250 nM) over cysteine (Fig. 4e, g), while IMCC26103 preferred cysteine (optimum at 10 nM) over methionine (Fig. 4f, 4h), which was difficult to predict from genome information. Although a limited number of substrates was tested, these differential preferences of different acI tribes on growth substrates may lead to niche differentiation, underlying the tribe-specific spatiotemporal dynamics of the acI lineage found in several cultivation-independent studies[16,28-30].

In conclusion, we successfully maintained actively-growing pure cultures of the acI lineage, the most abundant freshwater bacterioplankton group, by supplementing catalase into the culture media to lower H_2O_2 concentration, enabling further analysis of the physiological properties that could not be inferred from genome sequences alone. It is expected the simple catalase-supplement method can accelerate the cultivation of bacterioplankton with streamlined genomes and thus contribute to studies on the ecological roles of ubiquitous and abundant freshwater oligotrophic bacteria.

Methods

bioRxiv preprint doi: https://doi.org/10.1101/343640; this version posted June 11, 2018. The copyright holder for this preprint (which was not certified by peer review) is the author/funder, who has granted bioRxiv a license to display the preprint in perpetuity. It is made available under aCC-BY-NC 4.0 International license.

Initial isolation of the acI stains, medium preparation, and revival experiments

Freshwater collection, initial isolation, and identification of strains IMCC25003 and IMCC26103 are described in our previous study[9]. Briefly, both strains were initially isolated as liquid cultures by high-throughput culturing (HTC) method based on dilution-to-extinction in 0.2 μm-filtered and autoclaved freshwater media supplemented with very low levels of carbon compounds, amino acids mixture, and vitamin mixture. Two cryovials each containing 200 μl of initial HTC cultures suspended in 10% (v/v) sterile glycerol were stored at -80°C and used for further revival experiments. As shown in Supplementary Fig. 2, the axenic culture of IMCC25003 was obtained from the revival experiments, which was further used in the following experiments to establish a stably-maintainable pure culture of IMCC25003.

Culture media for reviving IMCC25003 were prepared based on natural freshwater (*see* Supplementary Table 1 for culture media ingredients). Natural freshwater collected at a depth of 1 m from the Dam station (37°56′50.6″ N, 127°49′7.9″ E) of Lake Soyang in February 2016 was filtered through a 0.2 μm pore-size membrane filter (Supor, Pall Corporation), autoclaved for 1.5 h, and aerated for 3 h. The filtered-autoclaved-aerated medium was supplemented with 10 μM NH_4Cl, 10 μM KH_2PO_4, and trace metal mixture[31], which was designated FAM (filtered and autoclaved freshwater medium). The FAM medium supplemented with the vitamin mixture[32] (Supplementary Table 1), designated FAMV, was used as a basal medium that did not contain extra-amended organic compounds. The FAMV supplemented with a carbon mixture (CM; 50 μM pyruvate, 5 μM D-glucose, 5 μM N-acetyl-D-glucosamine, 5 μM D-ribose, and 5 μM methyl alcohol) and amino acid mixture (AA; 20 proteinogenic amino acids, 100 nM each) were prepared and used as the basal heterotrophic growth medium.

As the first attempt to obtain a stable culture of IMCC25003 (Supplementary Table 2), 100 μl glycerol stock of IMCC25003 was inoculated into 20 ml of FAMV, FAMV amended with CM (FAMV+CM), FAMV amended with AA (FAMV+AA), and FAMV amended with CM and AA (FAMV+CM+AA). Different concentrations (0.5×, 1×, 5×, and 10×) of CM were added to FAMV+AA and the growth of IMCC25003 was tested. A 0.1 μm-filtered but non-autoclaved freshwater medium (FM) and artificial freshwater medium (AFM)[19] each supplemented with vitamin mixture, CM, and AA were also tested. In the second attempt, the following organic nutrients were individually supplemented into FAMV+CM+AA: 20 μM acetate, 20 μM oxaloacetate, 20 μM putrescine, 20 μM glycerol, 20 μM xylose, 1 mg l^{-1} proteose peptone, and 1 mg l^{-1} yeast extract. In the third attempt, the spent medium of the genus *Limnohabitans* which is often considered as a co-occurring bacterium

bioRxiv preprint doi: https://doi.org/10.1101/343640; this version posted June 11, 2018. The copyright holder for this preprint (which was not certified by peer review) is the author/funder, who has granted bioRxiv a license to display the preprint in perpetuity. It is made available under aCC-BY-NC 4.0 International license.

with acI bacteria, was added to the growth test medium. *Limnohabitans* sp. IMCC26003 grew to 3.1×10^6 cells ml^{-1} in 100 ml of FAMV+CM+AA at 25°C for 2 weeks. After the *Limnohabitans* culture was filtered through a 0.2 μm pore-size membrane followed by a 0.1 μm pore-size membrane, 1 ml of the filtrate of the spent medium and 100 μl of glycerol stock of IMCC25003 were inoculated into 20 ml of FAMV+CM+AA. In the fourth attempt, catalase (from bovine liver, C9322, Sigma-Aldrich) stock solution (10^5 U ml^{-1} in 10 mM PBS, pH 7.4) was added to FAMV+CM+AA at a final concentration of 10 U ml^{-1} and 100 μl glycerol stock of IMCC25003 was inoculated. All reviving tests were performed at 18°C for 5 weeks.

Measurement of bacterial cell densities

Bacterial cell densities in all growth experiments were determined by flow cytometry (Guava easyCyte Plus, Millipore) as described previously[31,33]. After 200 μl of bacterial cultures were stained with SYBR Green I (5× final concentration, Invitrogen) for 1 h, each stained sample was run for 10 s or until total cell counts reached 5000. To accurately measure the cell counts in the samples with high cell density, the stained sample was diluted to contain less than 200 cells μl^{-1}.

Culture maintenance and confirmation of culture purity

Bacterial cultures of strains IMCC25003 and IMCC26103 revived first from glycerol stocks by catalase amendment were purified twice by dilution-to-extinction culturing using FAMV+CM+AA containing 10 U ml^{-1} of catalase. Cells were diluted to 5, 1, or 0.1 cells ml^{-1} and dispensed into 48-well plates (1 ml per each well). After incubation, growth-positive wells (>10^5 cells ml^{-1}) from the most diluted inoculum (0.1 cells ml^{-1}) were used for next round of dilution-to-extinction, resulting in the establishment of stably-growing pure cultures.

To confirm the purity of the established pure cultures by FISH, 5 ml of exponentially grown cells were fixed with 2% paraformaldehyde (in PBS, pH 7.4) and filtered through 0.2-μm polycarbonate filters (Isopore, Millipore). Hybridization was performed at 35°C for 6 h in hybridization buffer [900 mM NaCl, 20 mM Tris (pH 7.4), 0.01% SDS, 15% formamide] with Cy3-labeled oligonucleotide probes (AcI-852 and AcI-1214; 2 ng μl^{-1} each) and helper probes (AcI-852-H1 and AcI-852-H2; 2 ng μl^{-1} each) targeting the acI clade[6]. After washing the membranes twice with washing buffer [150 mM NaCl, 20 mM Tris (pH 7.4), 6 mM EDTA, and 0.01% SDS] at

bioRxiv preprint doi: https://doi.org/10.1101/343640; this version posted June 11, 2018. The copyright holder for this preprint (which was not certified by peer review) is the author/funder, who has granted bioRxiv a license to display the preprint in perpetuity. It is made available under aCC-BY-NC 4.0 International license.

55°C for 10 min followed by DAPI (4,6-diamidino-2-phenylindole) staining, Cy3-positive and DAPI-positive cells were visualized with a confocal laser scanning microscope (LSM 510 META, Carl Zeiss).

For purity confirmation by genome sequencing, the two strains were cultivated in 4 L of FAMV+CM+AA supplemented with 10 U ml^{-1} of catalase. Cells were harvested by centrifugation at 20,000 ×*g* for 120 min and the cell pellets (Supplementary Fig. 4a) were used for genomic DNA extraction. Sequencing libraries were constructed using the Nextera library preparation kit. Genome sequencing was performed on an Illumina MiSeq platform (2 × 300 bp) by ChunLab, Inc (Seoul, Republic of Korea). Raw sequencing data were assembled using SPAdes 3.9.0[34], resulting in a circularly closed complete genome for both strains. Comparison of the genome sequences obtained in this study to those obtained by MDA[9] was performed using BLASTn. Calculation of sequencing coverages and estimation of culture purity based on reads mapping were performed as described by Kang *et al.*[9], using the 'depth' and 'flagstat' options in samtools.

After purification, both strains were stored as 10% (v/v) glycerol suspensions at -80°C and working cultures were maintained in FAMV+CM+AA supplemented with 1 U ml^{-1} of catalase at 25°C. Throughout this study, the peak shape of the cultures in the flow cytometry, morphology of SYBR Green I-stained cells in epifluorescence microscopy, FISH images obtained using acI-specific probes, and electropherograms from 16S rRNA gene sequencing were routinely examined to evaluate culture purity.

Characterization of catalase-dependent growth properties

The effects of catalase concentration on the growth of strains IMCC25003 and IMCC26103 were tested in triplicate in FAMV+CM+AA supplemented with 0.5, 1, 5, 10, and 20 U ml^{-1} of catalase at 25°C. Bacterial cell densities were measured by flow cytometry every 2 d.

To confirm the effect of catalase on the enhancement of cellular growth and decrease of H_2O_2 concentration, 10 U ml^{-1} of catalase was added to IMCC25003-inoculated culture medium (FAMV+CM+AA) that had been maintained for 0, 7, and 13 days without catalase treatment. Similarly, for strain IMCC26103, 10 U ml^{-1} of catalase was spiked at 0, 5, and 12 days. Cultures maintained without catalase were used as controls. For all cultures, cell densities were monitored every day by flow cytometry. At the same time, the concentration of H_2O_2 in the culture medium was measured using a modified acridinium ester chemiluminescence method[35] described below.

bioRxiv preprint doi: https://doi.org/10.1101/343640; this version posted June 11, 2018. The copyright holder for this preprint (which was not certified by peer review) is the author/funder, who has granted bioRxiv a license to display the preprint in perpetuity. It is made available under aCC-BY-NC 4.0 International license.

274

275 **Determination of hydrogen peroxide concentration**

276 A modified acridinium ester chemiluminescence method[35] was applied to determine H_2O_2 concentrations in
277 the culture medium. To measure H_2O_2 concentrations at the nanomolar level, acridinium NHS ester (A63063;
278 Cayman Chemical) reagent was used as an indicator and the resulting chemiluminescence was estimated using a
279 SpectraMax L microplate Reader (Molecular Devices). A standard curve for H_2O_2 was prepared in the range of
280 0.02–2.0 µM by diluting 30% (v/v) of H_2O_2 solution (H1009; Sigma-Aldrich) with ddH_2O. The acridinium ester-
281 H_2O_2 response signal was integrated for 13 s after sequential injections of 20 µl 2 M Na_2CO_3 (pH 11.3) followed
282 by 80 µl of 2.2 mg L^{-1} acridinium ester (in 1 mM phosphate buffer, pH 3) at 300 µl s^{-1} injection flow speed and
283 0.1-s interval. All measurements were conducted in triplicate at 20°C.

284

285 **Morphological and physiological characterization of acI strains**

286 Cell morphology was examined by transmission electron microscopy (CM200, Philips) using whole cell
287 staining and thin-sectioning. For whole cell staining, 20 ml cultures were gently filtered using a 0.2-µm pore size
288 polycarbonate membrane on which formvar/carbon-coated copper grids were placed, followed by staining of the
289 grids with 0.5% uranyl acetate. To prepare thin-sectioned samples, cell pellets were harvested by centrifugation
290 of 2 L cultures at 20,000 ×*g* for 120 min. Cell pellets that were primary fixed with 2.0% Karnovsky's fixative and
291 secondary fixed with 1.0% osmium tetroxide were dehydrated using ethanol series from 35% to 100% and Epon
292 812 resin was infiltrated. Ultrathin sections (70 nm) were prepared with an ultramicrotome using a diamond
293 knife, placed on formvar/carbon-coated copper grids, and double-stained with 2% uranyl acetate and 0.5% lead
294 oxide.

295 The temperature range for growth of the two acI strains was monitored at 10–35°C in FAMV+CM+AA
296 supplemented with 10 U ml^{-1} of catalase. After the optimum temperature had been determined, all growth
297 experiments were performed in triplicate at 25°C in different growth media supplemented with 10 U ml^{-1} of
298 catalase. The growth curves in FAMV, FAMV+CM, FAMV+AA, and FAMV+CM+AA were determined to
299 evaluate the effects of carbon compound mixtures and amino acids mixtures on cellular growth. To identify
300 which amino acids are required for growth, 20 individual amino acids were supplemented in the FAMV medium
301 at 100 nM and cellular growth was monitored. Similarly, 5 individual carbon sources (50 µM pyruvate, 5 µM D-

bioRxiv preprint doi: https://doi.org/10.1101/343640; this version posted June 11, 2018. The copyright holder for this preprint (which was not certified by peer review) is the author/funder, who has granted bioRxiv a license to display the preprint in perpetuity. It is made available under aCC-BY-NC 4.0 International license.

glucose, 5 μM *N*-acetyl-D-glucosamine, 5 μM D-ribose, and 5 μM methyl alcohol) were supplemented into FAMV+AA and the growth curves were determined. To determine the optimal concentration of reduced sulfur compounds, growth of the acI strains was measured at 0–10 μM of methionine (for IMCC25003) and cysteine (for IMCC26103).

Cellular fatty acid profiles were determined using the cells harvested from 2 L cultures grown in FAMV+CM+AA supplemented with 10 U ml^{-1} of catalase. Fatty acid methyl esters were extracted from cell pellets using the standard protocol for the Sherlock Microbial Identification System (MIDI, Inc.A) and analyzed by gas chromatography (Agilent 7890 GC) based on MIDI version 6.1 with the TSBA6 database[36].

Measurement of *katG* expression by qPCR

Strain IMCC25003 was grown in triplicate in 4 L of FAMV+CM+AA supplemented with 1 U ml^{-1} of catalase until the early stationary phase. Each 4-L bacterial culture was harvested by centrifugation at 20,000 ×*g* for 120 min. To examine the expression of IMCC25003 *katG* and compare relative level of gene expression according to H_2O_2 concentrations, harvested cells were treated with different concentrations of H_2O_2 (10, 50, and 100 μM) for 30 min and untreated cells were used as a control. RNA was extracted using TRIzol (Sigma-Aldrich). Reverse transcription was performed with 1 μg of RNA using qPCRBIO cDNA Synthesis Kit (PCRBIO Systems) and real-time qPCR was conducted using qPCRBIO SyGreen Blue Mix Lo-ROX (PCRBIO Systems) in a real-time thermal cycler (Rotor-Gene 3000, Corbett). The *katG* primer set (forward, 5′-CATGGCGATGAATGATGAAG-3′; reverse, 5′-GCTGTTCTTCCAGCCAAGTC-3′) for targeting *katG* of IMCC25003 was used to evaluate gene expression and the GAPDH gene of IMCC25003 was employed as a housekeeping gene with the GAPDH primer set (forward, 5′-GTTCAGCGACAGACCTCACA-3′; reverse, 5′-TGGTGAGCTGTGAATCGAAG-3′).

Expression, purification, and characterization of KatG from IMCC25003

The gene encoding catalase-peroxidase (KatG) of IMCC25003 was amplified by PCR using the following primers: forward, 5′-CATATGATGACTCAAGAATCAACTCC-3′; reverse, 5′-CTCGAGTTACTTCTTCTTTGAC-3′. The PCR product was inserted into the pET-15b vector (Novagen) and expressed in *Escherichia coli* BL21 (DE3) using 1 mM isopropyl-*β*-D-thiogalatoside (Sigma-Aldrich). The

bioRxiv preprint doi: https://doi.org/10.1101/343640; this version posted June 11, 2018. The copyright holder for this preprint (which was not certified by peer review) is the author/funder, who has granted bioRxiv a license to display the preprint in perpetuity. It is made available under aCC-BY-NC 4.0 International license.

expressed KatG-His recombinant protein was purified using a gravity-flow Ni^{2+}-nitrilotriacetic acid affinity column (Novagen). The high concentration of salts used for elution in the affinity column was removed using a PD-10 desalting column (GE Healthcare). To increase protein purity, the eluted fractions were applied to a Superose-12 FPLC column (10 × 300 mm, GE Healthcare) equilibrated with 50 mM potassium phosphate buffer (pH 7.0). The purified recombinant proteins were concentrated to approximately 10 mg ml^{-1} in Centricon tubes (MWCO 10,000 Da; Millipore) and stored at 4°C. All purification steps were carried out at 4°C or on ice.

The native molecular weight of IMCC25003 KatG was determined by size exclusion chromatography on a Superose-12 FPLC column (10 × 300 mm, GE Healthcare) equilibrated with 50 mM potassium phosphate buffer (pH 7.0). The molecular weights of the subunits were determined by discontinuous sodium dodecyl sulfate-polyacrylamide gel electrophoresis (SDS-PAGE) according to the standard Laemmli method. Catalytic activity of recombinant IMCC25003 KatG was determined using a spectrophotometric assay by measuring the decomposition of H_2O_2 at 240 nm. Catalase-specific activity was quantified by allowing varying amounts of enzyme (0–1.0 µg for bovine catalase; 0–5.0 µg for IMCC25003 KatG) to react with 5 mM H_2O_2 in 50 mM potassium phosphate buffer (pH 7.0) at 25°C. The absorption coefficient at 240 nm, pH 7.0, and 25°C for H_2O_2 was determined to be 49.8 M^{-1} cm^{-1}. Kinetic parameters were determined in triplicate from initial linear reaction rates of H_2O_2 ranging from 1 to 10 mM. The apparent Km (mM) and kcat (s^{-1}) values at these substrate concentrations were determined from Lineweaver-Burk plots. Catalase from bovine liver was used as a positive control. In SDS-PAGE, staining for catalase activity was performed with the ferricyanide negative staining method using 2% (w/v) ferric chloride and 2% (w/v) potassium ferricyanide solution, and peroxidase activity was detected by double-staining with 3,3′,5,5′-tetramethylbenzidine[37].

Phylogenetic analyses based on 16S rRNA gene, whole genome, and KatG protein

The 16S rRNA gene sequences of the acI genomes[8-10] were downloaded from the IMG database and GenBank, aligned using SINA online aligner, and imported into the ARB-SILVA database (SSURef NR 99, release 123). Multiple alignments of the imported sequences and other reference sequences of the acI lineage were exported with the 'ssuref:bacteria' filter and used to construct a maximum-likelihood tree in RAxML 8.2.7 with the GTRGAMMA model. Phylogenetic assignment of the sequences was performed as described by Newton *et al*.[5] and the recently proposed names for the two *Candidatus* genera[10] .

bioRxiv preprint doi: https://doi.org/10.1101/343640; this version posted June 11, 2018. The copyright holder for this preprint (which was not certified by peer review) is the author/funder, who has granted bioRxiv a license to display the preprint in perpetuity. It is made available under aCC-BY-NC 4.0 International license.

To build phylogenomic trees, protein sequences predicted in 4 completed acI genomes[9] and single-cell genomes[8] and 16 recently published acI genomes[10] were downloaded from the IMG database and NCBI RefSeq database. Downloaded protein sequences were processed using CheckM[38], which produces concatenated alignment of 43 conserved proteins. This concatenated alignment was used to build a maximum-likelihood tree using RAxML 8.2.7 with the PROTGAMMAAUTO model.

KatG proteins in the acI genomes (listed in Supplementary Table 4) were searched by BLASTp using the KatG sequence of IMCC25003 as a query and the acI protein sequences downloaded above as a search database, which resulted in the identification of a total of 20 acI KatG proteins. Phylogenetic trees of KatG proteins were constructed to identify the phylogenetic positions of the KatGs found in the acI genomes. Sequences collected for tree construction included the following: 20 acI KatG proteins, 16 KatG proteins showing high similarities to acI KatG proteins in BLASTp against the nr database of GenBank, 19 actinobacterial KatG proteins searched from the genomes representing diverse taxonomic groups of the phylum *Actinobacteria*[9], and >300 KatG proteins downloaded from PeroxiBase[39] (http://peroxibase.toulouse.inra.fr; Category 'Catalase peroxidase' of 'Class I peroxidase superfamily' under 'Non Animal peroxidase'). After sequence collection, several rounds of alignment and tree building were performed, and some sequences were excluded because of their short length, poor alignment, or unstable positioning. Finally, 303 KatG proteins were selected, aligned with Muscle[40] implemented in the MEGA 6 program, and used to construct a maximum likelihood tree using RAxML (version 8.2.7), with automatic model selection based on the aic criterion (-m PROTGAMMAAUTO --auto-prot=aic). The selected model was LG likelihood with empirical base frequencies. Grouping of the KatG proteins was performed as described by Zamocky *et al.*[27]

Data availability

The complete genome sequences of strains IMCC25003 and IMCC26103 obtained from cell pellets using Illumina MiSeq platform have been deposited in GenBank with the accession numbers CP029557 for IMCC25003 and CP029558 for IMCC26103.

Acknowledgements

bioRxiv preprint doi: https://doi.org/10.1101/343640; this version posted June 11, 2018. The copyright holder for this preprint (which was not certified by peer review) is the author/funder, who has granted bioRxiv a license to display the preprint in perpetuity. It is made available under aCC-BY-NC 4.0 International license.

This study was supported by the Mid-Career Research Program through the National Research Foundation (NRF) funded by the Ministry of Sciences and ICT (to J-CC, NRF-2016R1A2B2015142) and partially by the Basic Science Research Program funded by the Ministry of Education, Republic of Korea (to IK, NRF-2016R1A6A3A11934789; to J-HS, NRF-2016R1A6A3A11935361).

Author contributions

S.K isolated and physiologically characterized strains IMCC25003 and IMCC26103. S.K and I.K analyzed the genome sequences and phylogeny. J.-H.S performed the experiments for the expression and characterization of KatG from IMCC25003. J.-C.C. and I.K designed and supervised the study. S.K, I.K., J.-H.S, and J.-C.C. wrote the manuscript.

Competing interests

The authors declare no competing interests.

bioRxiv preprint doi: https://doi.org/10.1101/343640; this version posted June 11, 2018. The copyright holder for this preprint (which was not certified by peer review) is the author/funder, who has granted bioRxiv a license to display the preprint in perpetuity. It is made available under aCC-BY-NC 4.0 International license.

399 # Figures

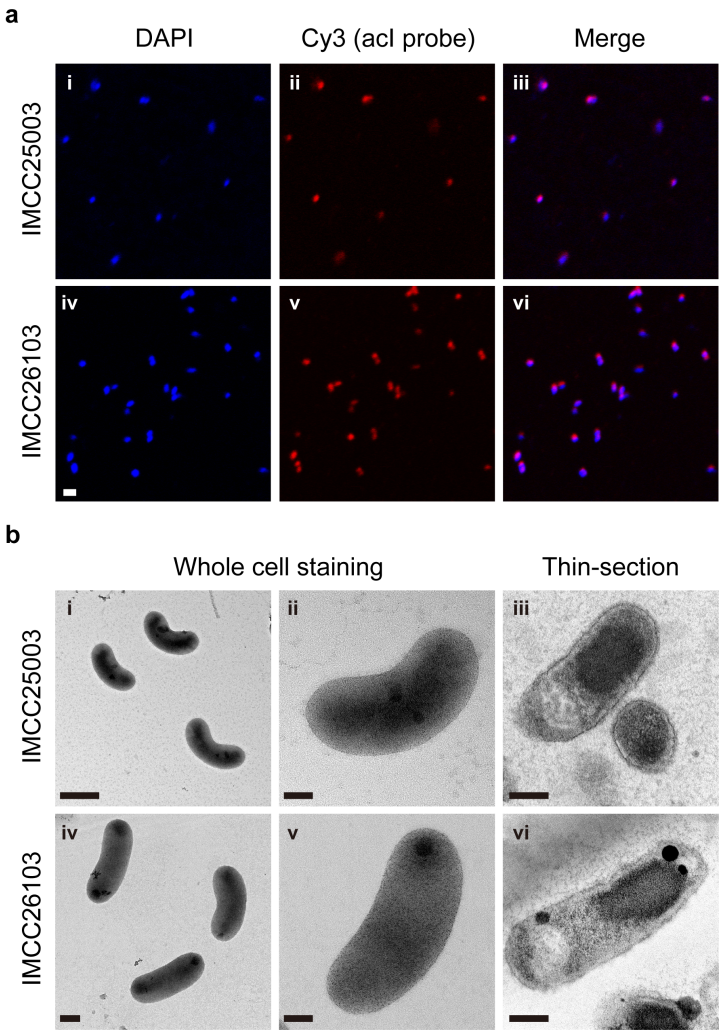

400

401 **Figure 1.** Microscopic examination of the two acI strains for purity evaluation and morphological
402 characterization. (a) Demonstration of culture purity of strains IMCC25003 (upper; i, ii, and iii) and IMCC26103
403 (lower; iv, v, and vi) by FISH analysis. The acI cells were dual-stained with DAPI (i and iv) and Cy3-conjugated
404 oligonucleotide probes specific to the acI lineage (AcI-852 and AcI-1214) (ii and v). Merged images are shown
405 in iii and vi. Bar, 1 μm. (b) Cell morphology of strains IMCC25003 (upper; i, ii, and iii) and IMCC26103 (lower;
406 iv, v, and vi) examined by transmission electron microscopy. The acI cells were stained with uranyl acetate (i, ii,
407 iv, and v) or double stained with uranyl acetate and lead oxide after thin-sectioning (iii and vi). Scale bars; 0.5
408 μm (i), 0.2 μm (iv), and 0.1 μm (ii, iii, v, and vi).

409

bioRxiv preprint doi: https://doi.org/10.1101/343640; this version posted June 11, 2018. The copyright holder for this preprint (which was not certified by peer review) is the author/funder, who has granted bioRxiv a license to display the preprint in perpetuity. It is made available under aCC-BY-NC 4.0 International license.

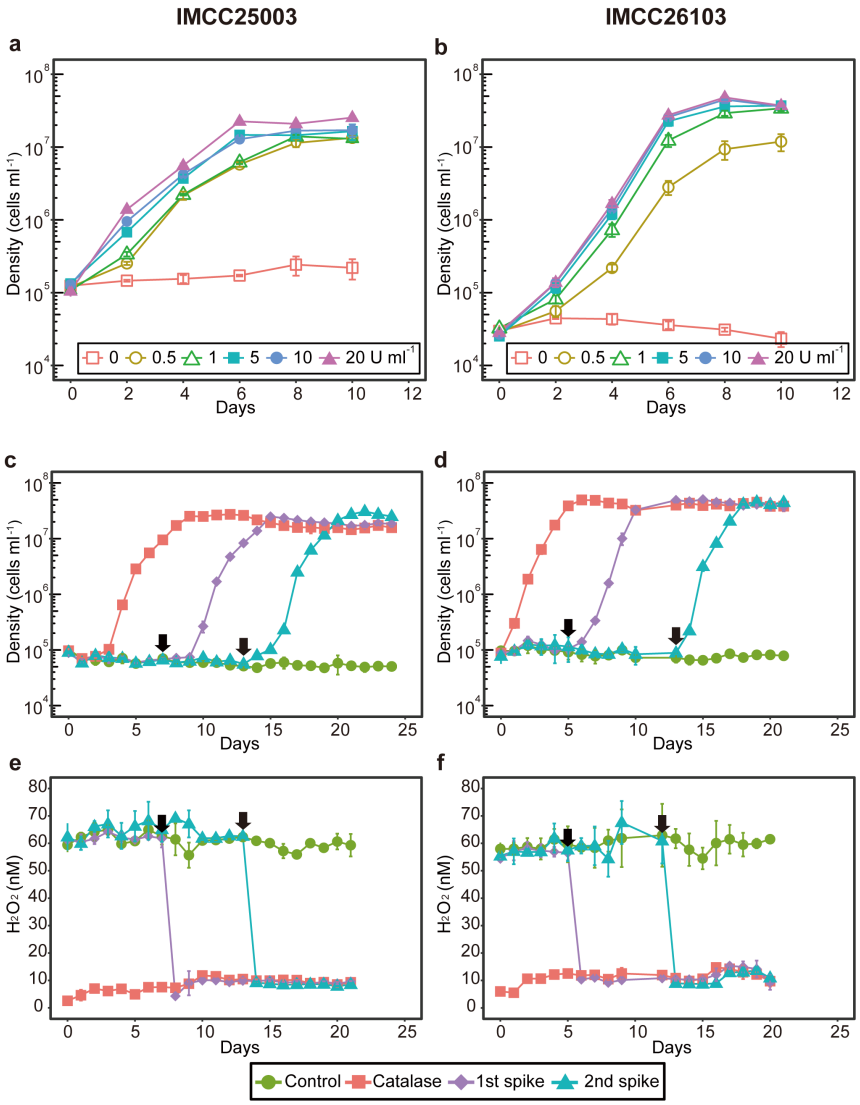

Figure 2. Catalase-dependent growth of the two acI strains. (a and b) The effect of various concentrations (0–20 U ml^{-1}) of catalase on the growth of strains IMCC25003 (a) and IMCC26103 (b). (c, d, e, and f) The effect of catalase addition on cell densities (c and d) and H_2O_2 concentrations (e and f) during cultivation of strains IMCC25003 (c and e) and IMCC26103 (d and f). Catalase (10 U ml^{-1}) was added to the culture media at day 0 ('Catalase') or days indicated by black arrows ('1st spike' and '2nd spike'). No catalase was added to the cultures designated 'Control'. All experiments were performed in triplicate using the culture medium FAMV+CM+AA (Supplementary Table 1). Error bars indicate standard deviation. Note that error bars shorter than the size of the symbols are hidden.

bioRxiv preprint doi: https://doi.org/10.1101/343640; this version posted June 11, 2018. The copyright holder for this preprint (which was not certified by peer review) is the author/funder, who has granted bioRxiv a license to display the preprint in perpetuity. It is made available under aCC-BY-NC 4.0 International license.

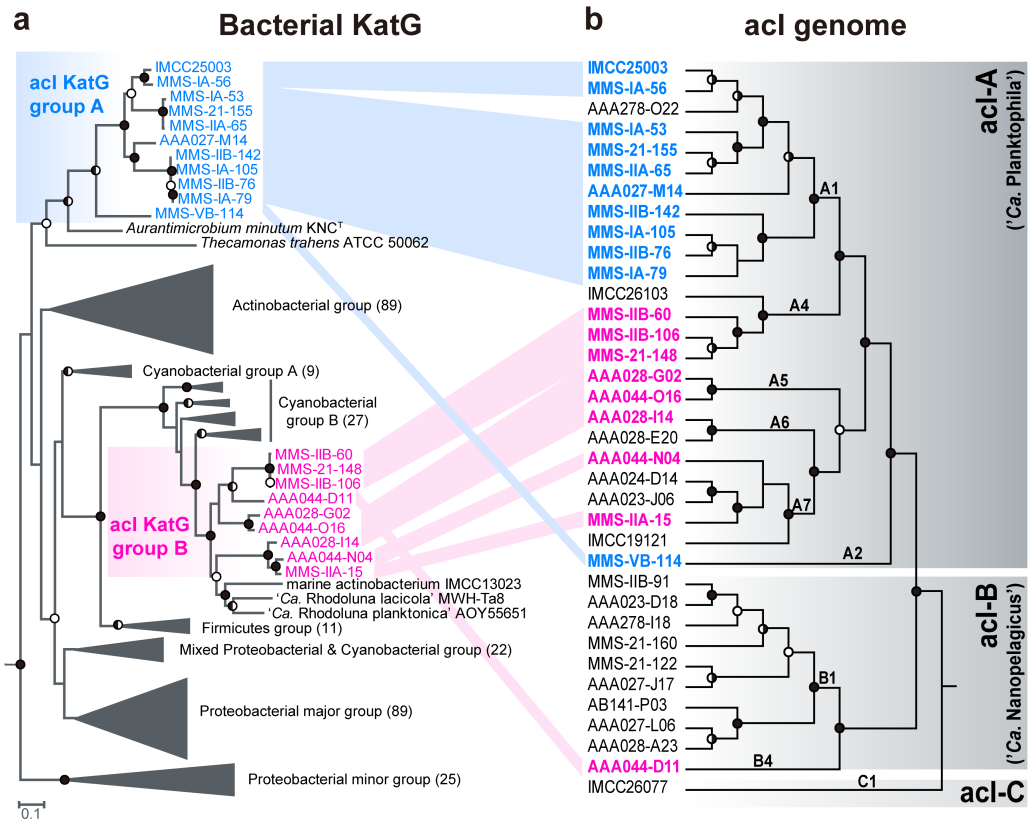

421

422 **Figure 3.** Comparison between a phylogenetic tree of bacterial KatG proteins and phylogenomic tree of
423 members of the acI lineage. (a) A maximum-likelihood tree of bacterial KatG protein sequences including those
424 predicted in the acI genomes. The acI KatG proteins are indicated in color (blue and red for acI KatG group A
425 and B, respectively), while other bacterial KatG proteins were grouped following the scheme proposed by
426 Zamocky *et al.*[27]. The number of proteins included in each KatG group are indicated within parentheses at the
427 end of group names. The KatG sequences of *Rhodopirellula baltica* and *Pirellula staleyi* (both from the phylum
428 *Planctomycetes*) were used as the outgroup. (b) A phylogenomic tree of members of the acI lineage constructed
429 using concatenated alignment of conserved marker proteins. The acI strains containing *katG* are indicated in
430 color according to the grouping in the left KatG tree. The SAG AAA027-D23 (belonging to the acSTL-A1
431 tribe)[16] was set as an outgroup. Only the tree topologies are shown, and branch lengths do not represent
432 phylogenetic distances. For both trees, bootstrap values (from 100 and 250 replicates for the KatG tree and
433 phylogenomic tree, respectively) are shown at the nodes as filled circles (≥90%), half-filled circles (≥70%), and
434 empty circles (≥50%).

435

bioRxiv preprint doi: https://doi.org/10.1101/343640; this version posted June 11, 2018. The copyright holder for this preprint (which was not certified by peer review) is the author/funder, who has granted bioRxiv a license to display the preprint in perpetuity. It is made available under aCC-BY-NC 4.0 International license.

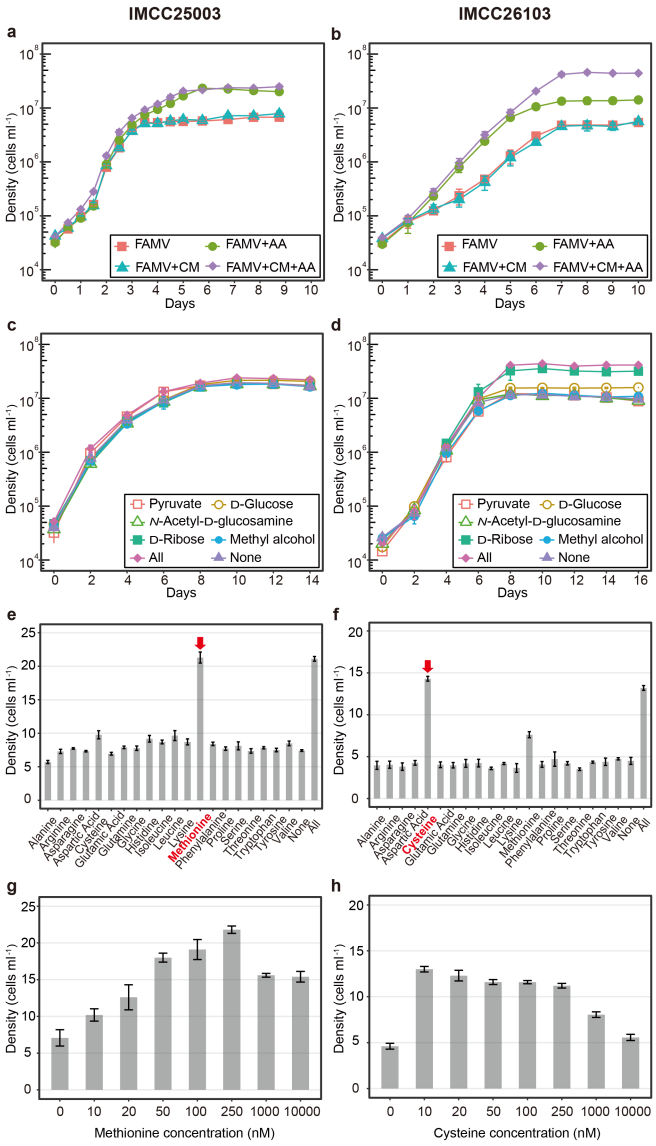

436

437 **Figure 4.** Effects of carbon sources and amino acids on the growth of the acI strains IMCC25003 (figures on the
438 left: a, c, e, and g) and IMCC26103 (figures on the right: b, d, f, and h). (a and b) The effects of amino acid
439 mixture (AA) and/or carbon source mixture (CM). AA and CM were added to the FAMV medium separately or
440 together. Detailed medium composition is presented in Supplementary Table 1. (c and d) The effects of
441 individual carbon compound. Each of 5 carbon compounds [5 μM, except for pyruvate (50 μM)] was added to
442 the FAMV+AA medium. All, 5 carbon substrates were added together; None, no carbon source was added. (e
443 and f) The effects of individual amino acids. Each of 20 proteinogenic amino acids was added at a concentration
444 of 100 nM to the basal medium FAMV. All, 20 amino acids were added together; None, no amino acid was
445 added. (g and h) Optimal concentrations of L-methionine (for IMCC25003) and L-cysteine (for IMCC26103).
446 Various concentrations (0–10,000 nM) of L-methionine or L-cysteine were added to the basal medium FAMV.

447

bioRxiv preprint doi: https://doi.org/10.1101/343640; this version posted June 11, 2018. The copyright holder for this preprint (which was not certified by peer review) is the author/funder, who has granted bioRxiv a license to display the preprint in perpetuity. It is made available under aCC-BY-NC 4.0 International license.

448 ## References

449 1. Moore, L. R., Rocap, G. & Chisholm, S. W. Physiology and molecular phylogeny of coexisting
450 *Prochlorococcus* ecotypes. *Nature* **393**, 464-467 (1998).

451 2. Rappe, M. S., Connon, S. A., Vergin, K. L. & Giovannoni, S. J. Cultivation of the ubiquitous SAR11
452 marine bacterioplankton clade. *Nature* **418**, 630-633 (2002).

453 3. Konneke, M. et al. Isolation of an autotrophic ammonia-oxidizing marine archaeon. *Nature* **437**, 543-
454 546 (2005).

455 4. Warnecke, F., Amann, R. & Pernthaler, J. Actinobacterial 16S rRNA genes from freshwater habitats
456 cluster in four distinct lineages. *Environ. Microbiol.* **6**, 242-253 (2004).

457 5. Newton, R. J., Jones, S. E., Eiler, A., McMahon, K. D. & Bertilsson, S. A guide to the natural history of
458 freshwater lake bacteria. *Microbiol. Mol. Biol. Rev.* **75**, 14-49 (2011).

459 6. Warnecke, F., Sommaruga, R., Sekar, R., Hofer, J. S. & Pernthaler, J. Abundances, identity, and growth
460 state of Actinobacteria in mountain lakes of different UV transparency. *Appl. Environ. Microbiol.* **71**,
461 5551-5559 (2005).

462 7. Allgaier, M. & Grossart, H.-P. Diversity and seasonal dynamics of *Actinobacteria* populations in four
463 lakes in northeastern Germany. *Appl. Environ. Microbiol.* **72**, 3489-3497 (2006).

464 8. Ghylin, T. W. et al. Comparative single-cell genomics reveals potential ecological niches for the
465 freshwater acl Actinobacteria lineage. *ISME J* **8**, 2503-2516 (2014).

466 9. Kang, I., Kim, S., Islam, M. R. & Cho, J.-C. The first complete genome sequences of the acI lineage,
467 the most abundant freshwater *Actinobacteria*, obtained by whole-genome-amplification of dilution-to-
468 extinction cultures. *Sci. Rep.* **7**, 42252 (2017).

469 10. Neuenschwander, S. M., Ghai, R., Pernthaler, J. & Salcher, M. M. Microdiversification in genome-
470 streamlined ubiquitous freshwater Actinobacteria. *ISME J* **12**, 185-198 (2018).

471 11. Jezbera, J., Sharma, A. K., Brandt, U., Doolittle, W. F. & Hahn, M. W. '*Candidatus* Planktophila
472 limnetica', an actinobacterium representing one of the most numerically important taxa in freshwater
473 bacterioplankton. *Int. J. Syst. Evol. Microbiol.* **59**, 2864-2869 (2009).

474 12. Garcia, S. L., McMahon, K. D., Grossart, H.-P. & Warnecke, F. Successful enrichment of the ubiquitous
475 freshwater acI *Actinobacteria*. *Environ. Microbiol. Rep.* **6**, 21-27 (2014).

bioRxiv preprint doi: https://doi.org/10.1101/343640; this version posted June 11, 2018. The copyright holder for this preprint (which was not certified by peer review) is the author/funder, who has granted bioRxiv a license to display the preprint in perpetuity. It is made available under aCC-BY-NC 4.0 International license.

13. Garcia, S. L. et al. Auxotrophy and intrapopulation complementary in the 'interactome' of a cultivated freshwater model community. *Mol. Ecol.* **24**, 4449-4459 (2015).

14. Morris, J. J., Lenski, R. E. & Zinser, E. R. The Black Queen Hypothesis: evolution of dependencies through adaptive gene loss. *mBio* **3**, e00036-12 (2012).

15. Giovannoni, S. J., Cameron Thrash, J. & Temperton, B. Implications of streamlining theory for microbial ecology. *ISME J* **8**, 1553-1565 (2014).

16. Garcia, S. L. et al. Contrasting patterns of genome-level diversity across distinct co-occurring bacterial populations. *ISME J* **12**, 742-755 (2018).

17. Konstantinidis, K. T. & Tiedje, J. M. Genomic insights that advance the species definition for prokaryotes. *Proc. Natl. Acad. Sci. USA.* **102**, 2567-2572 (2005).

18. Salcher, M. M., Posch, T. & Pernthaler, J. In situ substrate preferences of abundant bacterioplankton populations in a prealpine freshwater lake. *ISME J* **7**, 896-907 (2013).

19. Kim, S., Kang, I. & Cho, J. C. Genomic analysis of a freshwater actinobacterium, "*Candidatus* Limnosphaera aquatica" strain IMCC26207, isolated from Lake Soyang. *J. Microbiol. Biotechnol.* **27**, 825-833 (2017).

20. Morris, J. J., Kirkegaard, R., Szul, M. J., Johnson, Z. I. & Zinser, E. R. Facilitation of robust growth of *Prochlorococcus* colonies and dilute liquid cultures by "Helper" heterotrophic bacteria. *Appl. Environ. Microbiol.* **74**, 4530-4534 (2008).

21. Morris, J. J., Johnson, Z. I., Szul, M. J., Keller, M. & Zinser, E. R. Dependence of the cyanobacterium *Prochlorococcus* on hydrogen peroxide scavenging microbes for growth at the ocean's surface. *PLoS ONE* **6**, e16805 (2011).

22. Kim, J. G. et al. Hydrogen peroxide detoxification is a key mechanism for growth of ammonia-oxidizing archaea. *Proc. Natl. Acad. Sci. USA.* **113**, 7888-7893 (2016).

23. D'Souza, G. & Kost, C. Experimental evolution of metabolic dependency in bacteria. *PLoS Genet.* **12**, e1006364 (2016).

24. Morris, J. J., Papoulis, S. E. & Lenski, R. E. Coexistence of evolving bacteria stabilized by a shared Black Queen function. *Evolution* **68**, 2960-2971 (2014).

bioRxiv preprint doi: https://doi.org/10.1101/343640; this version posted June 11, 2018. The copyright holder for this preprint (which was not certified by peer review) is the author/funder, who has granted bioRxiv a license to display the preprint in perpetuity. It is made available under aCC-BY-NC 4.0 International license.

503 25. Desagher, S., Glowinski, J. & Premont, J. Pyruvate protects neurons against hydrogen peroxide-induced
504 toxicity. *J. Neurosci.* **17**, 9060-9067 (1997).
505 26. Varma, S. D. & Hegde, K. R. Lens thiol depletion by peroxynitrite. Protective effect of pyruvate. *Mol.*
506 *Cell. Biochem.* **298**, 199-204 (2007).
507 27. Zamocky, M., Gasselhuber, B., Furtmuller, P. G. & Obinger, C. Molecular evolution of hydrogen
508 peroxide degrading enzymes. *Arch. Biochem. Biophys.* **525**, 131-144 (2012).
509 28. Berry, M. A. et al. Cyanobacterial harmful algal blooms are a biological disturbance to Western Lake
510 Erie bacterial communities. *Environ. Microbiol.* **19**, 1462-2920 (2017).
511 29. Okazaki, Y. & Nakano, S.-I. Vertical partitioning of freshwater bacterioplankton community in a deep
512 mesotrophic lake with a fully oxygenated hypolimnion (Lake Biwa, Japan). *Environ. Microbiol. Rep.* **8**,
513 780-788 (2016).
514 30. Newton, R. J. & McLellan, S. L. A unique assemblage of cosmopolitan freshwater bacteria and higher
515 community diversity differentiate an urbanized estuary from oligotrophic Lake Michigan. *Front.*
516 *Microbiol.* **6**, 1028 (2015).
517 31. Carini, P., Steindler, L., Beszteri, S. & Giovannoni, S. J. Nutrient requirements for growth of the
518 extreme oligotroph '*Candidatus* Pelagibacter ubique' HTCC1062 on a defined medium. *ISME J* **7**, 592-
519 602 (2013).
520 32. Davis, H. C. & Guillard, R. R. L. Relative value of ten genera of micro-organisms as food for oyster
521 and clam larvae. *Fish. Bull. (Wash. D. C.).* **58,** 293–304 (1958).
522 33. Tripp, H. J. et al. SAR11 marine bacteria require exogenous reduced sulphur for growth. *Nature* **452**,
523 741-744 (2008).
524 34. Bankevich, A. et al. SPAdes: a new genome assembly algorithm and its applications to single-cell
525 sequencing. *J. Comput. Biol.* **19**, 455-477 (2012).
526 35. King, D. W. et al. Flow injection analysis of H_2O_2 in natural waters using acridinium ester
527 chemiluminescence: method development and optimization using a kinetic model. *Anal. Chem.* **79**,
528 4169-4176 (2007).
529 36. Sasser, M. *Identification of bacteria by gas chromatography of cellular fatty acids.* MIDI Technical
530 Note 101. Newark, DE: MIDI Inc. (1990).

bioRxiv preprint doi: https://doi.org/10.1101/343640; this version posted June 11, 2018. The copyright holder for this preprint (which was not certified by peer review) is the author/funder, who has granted bioRxiv a license to display the preprint in perpetuity. It is made available under aCC-BY-NC 4.0 International license.

37. Thomas, P. E., Ryan, D. & Levin, W. An improved staining procedure for the detection of the peroxidase activity of cytochrome P-450 on sodium dodecyl sulfate polyacrylamide gels. *Anal. Biochem.* **75**, 168-176 (1976).

38. Parks, D. H., Imelfort, M., Skennerton, C. T., Hugenholtz, P. & Tyson, G. W. CheckM: assessing the quality of microbial genomes recovered from isolates, single cells, and metagenomes. *Genome Res.* **25**, 1043-1055 (2015).

39. Fawal, N. et al. PeroxiBase: a database for large-scale evolutionary analysis of peroxidases. *Nucleic Acids Res.* **41**, D441-444 (2013).

40. Edgar, R. C. MUSCLE: multiple sequence alignment with high accuracy and high throughput. *Nucleic Acids Res.* **32**, 1792-1797 (2004).